

LA-UR-03-2005

Approved for public release;
distribution is unlimited.

Title: VACUUM, MATTER, ANTIMATTER AND THE PROBLEM
OF COLD COMPRESSION

Author(s): W. Greiner
T. Buervenich

Submitted to: Computational and Theoretical Methods in Nuclear Physics
Feb. 18-21, 2003
Playa del Carmen, Mexico

72



Los Alamos National Laboratory, an affirmative action/equal opportunity employer, is operated by the University of California for the U.S. Department of Energy under contract W-7405-ENG-36. By acceptance of this article, the publisher recognizes that the U.S. Government retains a nonexclusive, royalty-free license to publish or reproduce the published form of this contribution, or to allow others to do so, for U.S. Government purposes. Los Alamos National Laboratory requests that the publisher identify this article as work performed under the auspices of the U.S. Department of Energy. Los Alamos National Laboratory strongly supports academic freedom and a researcher's right to publish; as an institution, however, the Laboratory does not endorse the viewpoint of a publication or guarantee its technical correctness.

Computational and Group Theoretical Methods in Nuclear Physics
February 18-21, 2003
Playa del Carmen, Mexico

- Organizing Committee
- Advisory Committee
- Second circular
- Proceedings

JAMP



- Registration
- Accommodation
- Sponsors
- Conference photo

• **Scope of the symposium**

- SU(3) and Symplectic Models and their Applications**
- Pseudo-Spin in Nuclear Physics**
- Collective phenomena**
- Forum on physics outside academia**
- Computational Physics and Large-Scale Nuclear Models**
- Mathematical Physics**

VACUUM, MATTER, ANTIMATTER AND THE PROBLEM OF COLD COMPRESSION

W. GREINER

*Institut für Theoretische Physik, J.W. Goethe-Universität, D-60054 Frankfurt,
Germany*

T. BUERVENICH

*Theoretical Division, Los Alamos National Laboratory, Los Alamos, New Mexico
87545, USA*

We discuss the possibility of producing a new kind of nuclear system by putting a few antibaryons inside ordinary nuclei. The structure of such systems is calculated within the relativistic mean-field model assuming that the nucleon and antinucleon potentials are related by the G-parity transformation. The presence of antinucleons leads to decreasing vector potential and increasing scalar potential for the nucleons. As a result, a strongly bound system of high density is formed. Due to the significant reduction of the available phase space the annihilation probability might be strongly suppressed in such systems.

1. Introduction

In this proceedings article we would like to report on some recent exciting results that have been obtained together with our friends and collaborators I. N. Mishustin, L. M. Satarov, J. A. Maruhn, and H. Stöcker¹. Before embarking upon the physical discussion, we would like to introduce the ideas and the framework.

Presently it is widely accepted that the relativistic mean-field (RMF) model² gives a good description of nuclear matter and finite nuclei³. Within this approach the nucleons are supposed to obey the Dirac equation coupled to mean meson fields. Large scalar and vector potentials, of the order of 300 MeV, are necessary to explain the strong spin-orbit splitting in nuclei. The most debated aspect of this model is related to the negative-energy states of the Dirac equation. In most applications these states are simply ignored (no-sea approximation) or "taken into account" via the non-linear and derivative terms of the scalar potential. On the other

hand, explicit consideration of the Dirac sea combined with the G-parity arguments leads to such interesting conjectures as the existence of deeply-bound antinucleon states in nuclei ⁴ or even spontaneous production of nucleon-antinucleon pairs ^{5,6}. Unfortunately, the experimental information on the antinucleon effective potential in nuclei is obscured by the strong absorption caused by annihilation. The real part of the antiproton effective potential might be as large as 200–300 MeV, with the uncertainty reaching 100% in the deep interior of the nucleus.

Keeping in mind all possible limitations of the RMF approach, below we consider yet another interesting application of this model. Namely, we study properties of light nuclear systems containing a few real antibaryons. At first sight this may appear ridiculous because of the fast annihilation of antibaryons in the dense baryonic environment. But as our estimates show, due to a significant reduction of the available phase space for annihilation, the life time of such states might be long enough for their observation. In a certain sense, these states are analogous to the famous baryonium states in the $N\bar{N}$ system ⁷, although their existence has never been unambiguously confirmed. To our knowledge, up till now a self-consistent calculation of antinucleon states in nuclei has not been performed. Our calculations can be regarded as the first attempt to fill this gap. We consider first two nuclear systems, namely ¹⁶O and ⁸Be, and study the changes in their structure due to the presence of an antiproton. Then we discuss the influence of small antimatter clusters on heavy systems like ²⁰⁸Pb.

2. Theoretical framework

Below we use the RMF model which previously has been successfully applied for describing ground-states of nuclei at and away from the β -stability line. For nucleons, the scalar and vector potentials contribute with opposite signs in the central potential, while their sum enters in the spin-orbit potential. Due to G-parity, for antiprotons the vector potential changes sign and therefore both the scalar and the vector mesons generate attractive potentials.

To estimate uncertainties of this approach we use three different parametrizations of the model, namely NL3 ⁸, NL-Z2 ⁹ and TM1 ¹⁰. In this paper we assume that the antiproton interactions are fully determined by the G-parity transformation. We solve the effective Schrödinger equations for both the nucleons and the antiprotons. Although we neglect the Dirac sea polarization, we take into account explicitly the contribution of the an-

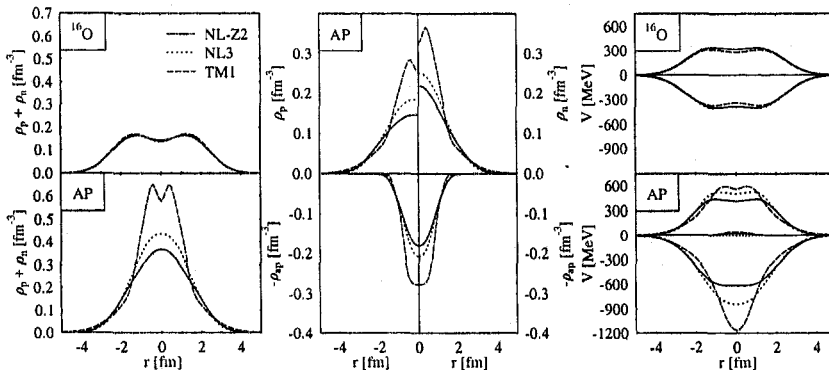


Figure 1. The left panel represents the sum of proton and neutron densities as function of nuclear radius for ^{16}O without (top) and with an antiproton (denoted by AP). The left and right parts of the upper middle panel show separately the proton and neutron densities, the lower part of this panel displays the antiproton density (with minus sign). The right panel shows the scalar (negative) and vector (positive) parts of the nucleon potential. Small contributions shown in the lower row correspond to the isovector (ρ -meson) part.

tibaryon into the scalar and vector densities. For protons and neutrons we include pairing correlations within the BCS model with a δ -force (volume pairing)¹¹. Calculations are done within the blocking approximation¹² for the antiproton, and assuming the time-reversal invariance of the nuclear ground-state. The coupled set of equations for nucleons, antinucleons and meson mean fields is solved iteratively and self-consistently. The numerical code employs axial and reflection symmetry, allowing for axially symmetric deformations of the system.

3. Structure of light nuclei containing antiprotons

As an example, we consider the nucleus ^{16}O with one antiproton in the lowest bound state. This nucleus is the lightest nucleus for which the mean-field approximation is acceptable, and it is included into the fit of the effective forces NL3 and NL-Z2. The antiproton state is assumed to be in the $s_{1/2}^+$ state. The antiproton contributes with the same sign as nucleons to the scalar density, but with opposite sign to the vector density. This leads to an overall increase of attraction and decrease of repulsion for all nucleons. The antiproton becomes very deeply bound in the $s_{1/2}^+$ state. To maximize attraction, protons and neutrons move to the center of the

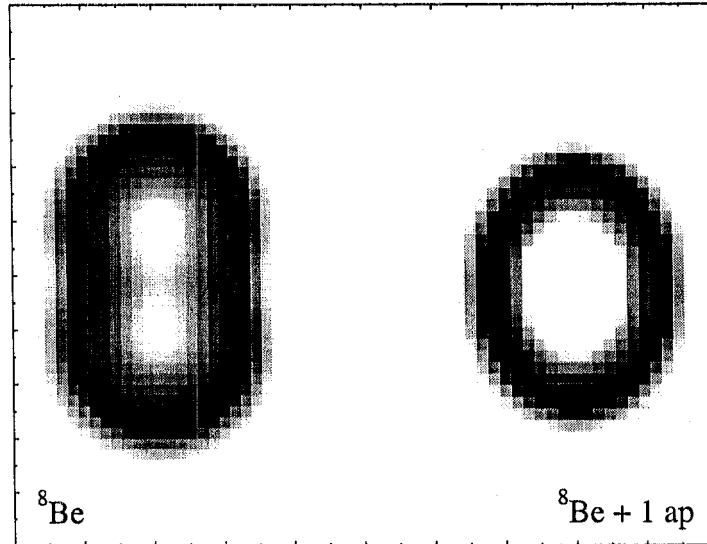


Figure 2. Contour plot of nucleon densities for ${}^8\text{Be}$ without (left) and with (right) antiproton calculated with the parametrization NL3. The maximum density of normal ${}^8\text{Be}$ is 0.20 fm^{-3} , while for the nucleus with the antiproton it is 0.61 fm^{-3} .

nucleus, where the antiproton has its largest occupation probability. This leads to a cold compression of the nucleus to a high density.

Figure 1 shows the densities and potentials for ${}^{16}\text{O}$ with and without the antiproton. For normal ${}^{16}\text{O}$ all RMF parametrizations considered produce very similar results. The presence of an antiproton dramatically changes the structure of the nucleus. The sum of proton and neutron densities reaches a maximum value of $(2 - 4) \rho_0$, where $\rho_0 \simeq 0.15 \text{ fm}^{-3}$ is the normal nuclear density, depending on the parametrization. The largest compression is predicted by the TM1 model. This follows from the fact that this parametrization gives the softest equation of state as compared to other forces considered here.

Since nucleons feel a deeper potential as compared to the nucleus without the antiproton, their binding energy increases too. The nucleon binding is largest within the NL3 parametrization. In the TM1 case, the $s_{1/2}^+$ state is also deep, but higher levels are less bound as compared to the NL3 and NL-Z2 calculations. This is a consequence of the smaller spatial extension of the potential in this case. The highest $s_{1/2}^-$ level is even less bound

than for the system without an antiproton. The total binding energy of the system is predicted to be 828 MeV for NL-Z2, 1051 MeV for NL3, and 1159 MeV for TM1. For comparison, the binding energy of a normal ^{16}O nucleus is 127.8, 128.7 and 130.3 MeV in the case of NL-Z2, NL3, and TM1, respectively. Due to this anomalous binding we call these systems Super Bound Nuclei (SBN).

As a second example, we investigate the effect of a single antiproton inserted into the ^8Be nucleus. In this calculation only the NL3 parametrization was used (the effect is similar for all three forces). The normal ^8Be nucleus is not spherical, exhibiting a clearly visible 2α structure with the deformation $\beta_2 \simeq 1.20$ in the ground-state. Inserting the antiproton gives rise to compression and change of nuclear shape. Its maximum density increases by a factor of three from 0.20 fm^{-3} to 0.61 fm^{-3} . The cluster structure of the ground state completely vanishes. A similar effect has been predicted in Ref. ¹³ for the case of the K^- bound state in the ^8Be nucleus. In our case the binding energy increases from 52.9 MeV (the experimental value is 56.5 MeV) to about 700 MeV!

4. Doubly-magic lead with antiproton and anti-alpha

We would like to discuss here the structural effect of an antiproton or an anti-alpha nucleus in the doubly magic lead nucleus. Contour plots of the sum of proton and neutron densities are shown in figures 3 (lead with an antiproton) and 4 (lead with an anti-alpha nucleus). In these cases we encounter a quite different scenario: again, the complete system is affected, but not in the sense that the whole nucleus shrinks and becomes very dense. Here, a small and localized region of high density develops within the heavy system. Additionally, the lead nucleus deforms itself. This effect is largest for the case of lead with $\bar{\alpha}$. The single-particle levels (Fig. 5) reflect this behaviour and indicate the cause for the deformation of lead: In a small region with a deep potential, only states with small angular momenta can be bound deeply. States with higher angular momenta do not have much overlap with the potential. This is exactly what can be concluded from Fig. 5. We see that basically only the lowest s - and p -states can be bound deeper than for lead without any antiparticles present. Higher lying states do not gain significantly binding or are even lesser bound.

The deformation effect probably has two reasons: firstly, a deformation might be energetically favourable to gain some binding for the higher lying states. Secondly, the distortion of the system due to the presence of

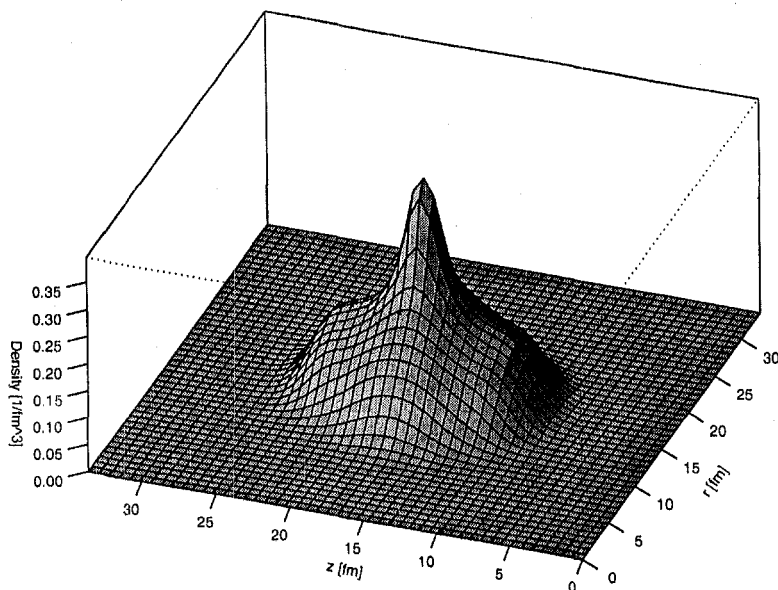


Figure 3. Surface plot of the sum of proton and neutron densities for the system ^{208}Pb with \bar{p} .

antiparticles destroys the magicity of the system.

5. Systems with total baryon number zero

It is interesting to consider finite systems having total baryon number zero, i.e. systems with the same amount of baryons and antibaryons. In the following we will present the cases of an α - anti- α and an ^{16}O - anti- ^{16}O system. Fig. 6 shows the results for a system consisting of an α - $\bar{\alpha}$ system. The total system possesses a quite small radius and large baryon and antibaryon densities. The total baryon density is exactly zero. Due

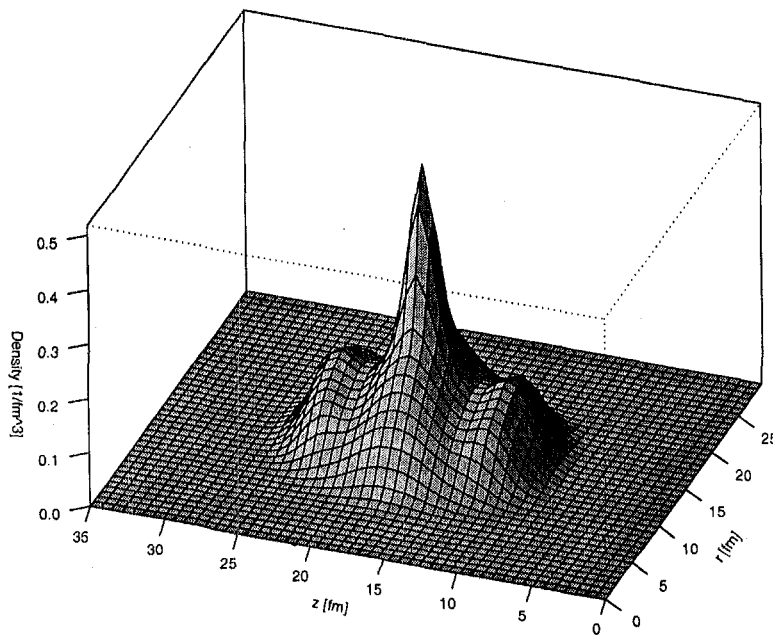


Figure 4. Surface plot of the sum of proton and neutron densities for the system ^{208}Pb with $\bar{\alpha}$.

to the inverse coupling of antibaryons to the vector field and the negative charge of the antibaryons, all sources and potentials except for the scalar one vanish completely! All particles occupy a single particle state with exactly the same energy, and they all feel the same potential, namely the scalar potential, to which all particles present in the system couple alike. The binding energy of this nuclear system is huge: 2649 MeV with the force NL3 and 2235 MeV with NL-Z2. This is about 100 times larger than the binding energy of one α .

A similar structural effect occurs for the system of ^{16}O - anti- ^{16}O .

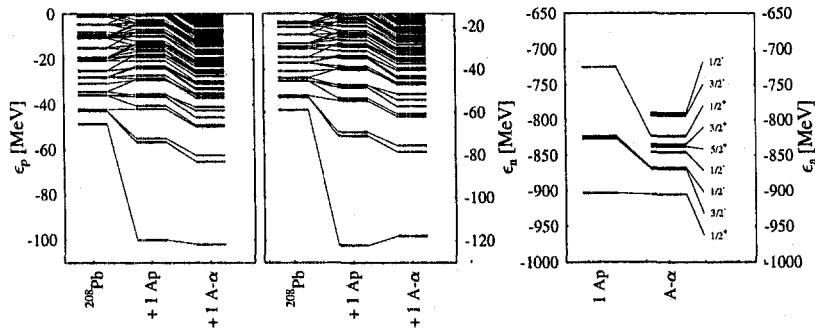


Figure 5. Single particle levels of protons (left), neutrons (middle) and antiproton levels (right) for the systems ^{208}Pb , $^{208}\text{Pb} + \bar{p}$ and $^{208}\text{Pb} + \bar{\alpha}$

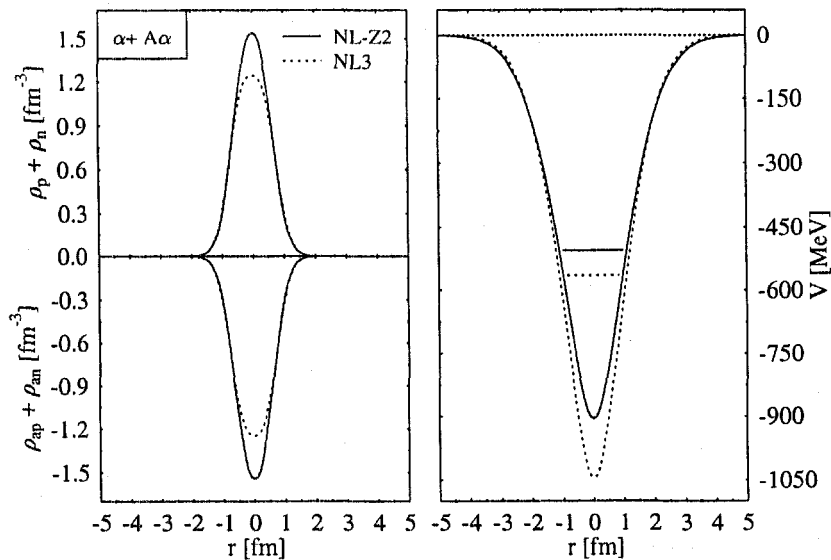


Figure 6. The left panel shows the sum of proton and neutron densities (top) as well as the corresponding sum for antibaryons for the α - $\bar{\alpha}$ system. The right panels shows the scalar potentials and the single particles levels of the nucleons and antinucleons.

Again, all potentials except the scalar one vanish exactly. The binding energy of this system is 13227 MeV with NL3. All nucleons and antinucleons reside in the lowest s- and p-levels. They are quite deeply bound (the

lowest $s_{1/2}$ levels is bound by about 750 MeV).

6. Life time, formation probability and signatures of SBNs

The crucial question concerning a possible observation of the SBNs is their life time. The only decay channel for such states is the annihilation on surrounding nucleons. The mean life time of an antiproton in nucleonic matter of density ρ_B can be estimated as $\tau = \langle \sigma_A v_{rel} \rho_B \rangle^{-1}$, where angular brackets denote averaging over the wave function of the antiproton and v_{rel} is its relative velocity with respect to nucleons. In vacuum the $N\bar{N}$ annihilation cross section at low v_{rel} can be parametrized as ¹⁴ $\sigma_A = C + D/v_{rel}$ with $C=38$ mb and $D=35$ mb. For $\langle \rho_B \rangle \simeq 2\rho_0$ this would lead to a very short life time, $\tau \simeq 0.7$ fm/c (for $v_{rel} \simeq 0.2$). However, one should bear in mind that the annihilation process is very sensitive to the phase space available for decay products. For a bound nucleon and antinucleon the available energy is $Q = 2m_N - B_N - B_{\bar{N}}$, where B_N and $B_{\bar{N}}$ are the corresponding binding energies. As follows from our calculations, this energy is strongly reduced compared to $2m_N$, namely, $Q \simeq 600 - 680$ MeV (TM1), 810–880 MeV (NL3) and 990–1050 MeV (NL-Z2) for the lowest antiproton states.

For such low values of Q many important annihilation channels involving two heavy mesons (ρ , ω , η , η' , ...) are simply closed. Other two-body channels such as $\pi\rho$, $\pi\omega$ are considerably suppressed due to the closeness to the threshold. As is well known, the two-pion final states contribute only about 0.4% of the annihilation cross section. Even in vacuum all above mentioned channels contribute to σ_A not more than 15% ¹⁵. Therefore, we expect that only multi-pion final states contribute significantly to antiproton annihilation in the SBN. But these channels are strongly suppressed due to the reduction of the available phase space. Our calculations show that changing Q from 2 GeV to 1 GeV results in suppression factors 5, 40 and 1000 for the annihilation channels with 3, 4 and 5 pions in the final state, respectively. Applying these suppression factors to the experimental branching ratios ¹⁶ we come to the conclusion that in the SBNs the annihilation rates can be easily suppressed by factor of 20–30. There could be additional suppression factors of a structural origin which are difficult to estimate at present. This brings the SBN life time to the level of 15–20 fm/c which makes their experimental observation feasible. The corresponding width, $\Gamma \sim 10$ MeV, is comparable to that of the ω -meson.

Let us discuss now how these exotic nuclear states can be produced in

the laboratory. We believe that the most direct way is to use antiproton beams of multi-GeV energy. This high energy is needed to suppress annihilation on the nuclear surface which dominates at low energies. To form a deeply bound state, the fast antiproton must transfer its energy and momentum to one of the surrounding nucleons. This can be achieved through reactions of the type $\bar{p}N \rightarrow B\bar{B}$ in the nucleus,

$$\bar{p} + (A, Z) \rightarrow B + \bar{B}(A - 1, Z'), \quad (1)$$

where $B = n, p, \Lambda, \Sigma$. The fast baryon B can be used as a trigger of events where the antibaryon \bar{B} is trapped in the nucleus. Obviously, this is only possible in inelastic $\bar{p}N$ collisions accompanied by the production of pions or particle-hole excitations. One can think even about producing an additional baryon-antibaryon pair and forming a nucleus with two antibaryons in the deeply bound states. In this case two fast nucleons will be knocked out from the nucleus.

Without detailed transport calculations it is difficult to find the formation probability, W , of final nuclei with trapped antinucleons in these reactions. A rough estimate can be obtained by assuming that antiproton stopping is achieved in a single inelastic collision somewhere in the nuclear interior i.e. taking the penetration length of the order of the nuclear radius R . From the Poisson distribution in the number of collisions the probability of such an event is

$$w_1 = \frac{R}{\lambda_{\text{in}}} \exp\left(-\frac{R}{\lambda}\right), \quad (2)$$

where $\lambda_{\text{in}}^{-1} = \sigma_{\text{in}}\rho_0$ and $\lambda^{-1} = (\sigma_{\text{in}} + \sigma_A)\rho_0$ (here σ_{in} and σ_A are the inelastic and annihilation parts of the $\bar{p}N$ cross section). The exponential factor in Eq. (2) includes the probability to avoid annihilation. For initial antiproton momenta $p_{\text{lab}} \simeq 10$ GeV we use $\sigma_{\text{in}} \simeq 25$ mb, $\sigma_A \simeq 15$ mb¹⁶ and get $\lambda \simeq 1.6$ fm which is comparable with the radii of light nuclei. For an oxygen target, using $R \simeq 3$ fm leads to $w_1 \simeq 0.17$.

In fact we need relatively small final antiproton momenta to overlap significantly with the momentum distribution of a bound state, namely, $\Delta p \sim \pi/R_{\bar{p}}$, where $R_{\bar{p}} \simeq 1.5$ fm is the characteristic size of the antiproton spatial distribution (see Fig. 1). The probability of such a momentum loss can be estimated by the method of Refs.^{17,18} which was previously used for calculating proton spectra in high-energy pA collisions. At relativistic bombarding energies the differential cross sections of the $\bar{p}p \rightarrow \bar{p}X$ and $pp \rightarrow pX$ reactions are similar. The inelastic parts of these cross sections drop rapidly with transverse momentum, but they are practically flat as

a function of longitudinal momentum of secondary particles. Thus, the probability of the final antiproton momentum to fall in the interval Δp is simply $\Delta p/p_{\text{lab}}$. For $p_{\text{lab}} = 10 \text{ GeV}$ and $\Delta p = 0.4 \text{ GeV}$ this gives 0.04. Assuming the geometrical fraction of central events $\sim 20\%$ we get the final estimate $W \simeq 0.17 \times 0.04 \times 0.2 \simeq 1.4 \cdot 10^{-3}$. One should bear in mind that additional reduction factors may come from the matrix element between the bare massive antibaryon and the dressed almost massless antibaryon in a deeply bound state. But even with extra factors $\sim 10^{-1} - 10^{-2}$ which may come from the detailed calculations the detection of SBNs is well within the modern experimental possibilities.

Finally, we mention a few possible signatures of SBNs which can be used for their experimental detection. First of all, we remind the reader that according to the Dirac picture, any real antibaryon should be interpreted as a hole in the otherwise filled Dirac sea. Therefore, the nucleons from the positive-energy states of the Fermi sea can make direct transitions to the vacant negative-energy states of the Dirac sea. These super-transitions will be accompanied by the emission of a single pion or kaon depending on the nature of the trapped antibaryon. The energy of such a super-transition is fixed by the discrete levels of the initial and final baryons and according to our calculations should be of about 1 GeV. Obviously, this emission should be isotropic in the rest frame of the nucleus. The 1-pion or 1-kaon annihilation is a unique feature of finite nuclear systems. In vacuum such transitions are forbidden by the energy-momentum conservation. Therefore, the observation of a line in the pion or kaon spectrum at energies between 1 and 2 GeV would be a clear signal of the deep antibaryon states in nuclei. One can also look for narrow photon lines with energies in the range from 40 to 200 MeV corresponding to the transitions of nucleons and antibaryons between their respective levels. It is interesting to note that these signals will survive even if due to the lack of time the nucleus does not fully rearrange to a new structure.

Another strong signal may come from the collective response of the target nucleus to the presence of an antibaryon. Initially the nucleons will acquire radial acceleration due to the attractive interaction with the trapped antibaryon. This will lead to a collective motion similar to monopole oscillations around the compressed SBN state. Moreover, annihilation of the antibaryon will leave the nuclear remnant in a nonequilibrium state of high density. The nuclear system will expand and eventually break up into fragments. Therefore, the decay of the SBN state will result in nuclear multifragmentation with large collective flow of fragments. Both proposed

signatures require rather ordinary measurements, which should be easy to perform with standard detectors.

7. Discussion and conclusions

Our main goal in this paper was to demonstrate that energetic antiproton beams can be used to study new interesting phenomena in nuclear physics. We discuss the possible existence of a completely new kind of strongly interacting systems where both the nucleons and the antinucleons coexist within the same volume and where annihilation is suppressed due to the reduction of the available phase space. Such systems are characterized by large binding energy and high nucleon density. Certainly, antinucleons can be replaced by antihyperons or even by antiquarks. We have presented the first self-consistent calculation of a finite nuclear system containing one antiproton in a deeply bound state. For this study we have used several versions of the RMF model which give excellent description of ordinary nuclei. The presence of an antiproton in a light nucleus like ^8Be or ^{16}O changes drastically the whole structure of the nucleus leading to a much more dense and bound state. In heavy systems the presence of a few antinucleons distorts and deforms the nuclear system leading to a localized central region of highly increased density. We find that that nuclear systems with total baryon number zero show extremely deep and symmetric states.

It is clear however that these structural changes can occur only if the life time of the antibaryons in the nuclear interior is long enough.

One should bear in mind that originally the RMF model was formulated within the Hartree and no-sea approximations. Implementing the Dirac sea may require serious revision of the model and inclusion of additional terms. Hartree calculations including the Dirac sea and Hartree-Fock calculations including exchange terms lead to smaller nucleon potentials in normal nuclei. Shallower potentials will produce smaller attraction for antinucleons, but the qualitative effect that the presence of antiprotons reduces repulsion and enhances attraction for nucleons will remain valid. We expect that the additional binding and compression of the nucleus will appear even for an antinucleon potential as low as 200 MeV.

In summary, on the basis of the RMF model we have studied the structure of nuclear systems containing a few real antibaryons. We have demonstrated that the antibaryons act as strong attractors for the nucleons leading to enhanced binding and compression of the recipient nucleus. As our estimates show the life times of antibaryons in the nuclear environment could

be significantly enhanced due to the reduction of the phase space available for annihilation. Narrow peaks in the pion or kaon spectra at the energy around 1 GeV are proposed as the most clear signature of deeply-bound antibaryon states in nuclei.

References

1. T. Bürvenich, I. N. Mishustin, L. M. Satarov, J. A. Maruhn, H. Stöcker, and W. Greiner, *Phys. Lett. B* **542** (2002) 261
2. B.D. Serot and J.D. Walecka, *Adv. Nucl. Phys.*, **16** (1985) 1.
3. P.G. Reinhard, *Rep. Prog. Phys.* **52** (1989) 439.
4. N. Auerbach, A.S. Goldhaber, M.B. Johnson, L.D. Miller, and A. Picklesimer, *Phys. Lett. B* **182** (1986) 221.
5. I.N. Mishustin, *Sov. J. Nucl. Phys.* **52** (1990) 722.
6. I.N. Mishustin, L.M. Satarov, J. Schaffner, H. Stöcker, and W. Greiner, *J. Phys. G* **19** (1993) 1303.
7. O.D. Dalkarov, V.B. Mandelzweig, and I.S. Shapiro, *Nucl. Phys. B* **21** (1970) 66.
8. G. Lalazissis, J. König, and P. Ring, *Phys. Rev. C* **55** (1997) 540.
9. M. Bender, K. Rutz, P.-G. Reinhard, J.A. Maruhn, and W. Greiner, *Phys. Rev. C* **60** (1999) 34304.
10. Y. Sugahara and H. Toki, *Nucl. Phys. A* **579** (1994) 557.
11. M. Bender, K. Rutz, P.-G. Reinhard, and J.A. Maruhn, *Eur. Phys. J. A* **8** (2000) 59.
12. K. Rutz, M. Bender, P.-G. Reinhard, J.A. Maruhn, and W. Greiner, *Nucl. Phys. A* **634** (1998) 67.
13. Y. Akaishi and T. Yamazaki, *Phys. Rev. C* **65** (2002) 044005.
14. C.B. Dover, T. Gutsche, M. Maruyama, and A. Faessler, *Prog. Part. Nucl. Phys.* **29** (1992) 87.
15. C. Amsler, *Rev. Mod. Phys.* **70** (1998) 1293.
16. J. Sedláč and V. Šimák, *Sov. J. Part. Nucl.* **19** (1988) 191.
17. R.C. Hwa, *Phys. Rev. Lett.* **52** (1984) 492.
18. L.P. Csernai and J.I. Kapusta, *Phys. Rev. D* **29** (1984) 2664.